Virchows Archiv (1995) 426:271–279

ORIGINAL ARTICLE

J. Miyagawa · M. Kuwajima · T. Hanafusa · K. Ozaki
H. Fujimura · A. Ono · R. Uenaka · I. Narama · T. Oue
K. Yamamoto · M. Kaidoh · H. Nikaido · J. Hayakawa
M. Horiuchi · T. Saheki · Y. Matsuzawa

Mitochondrial abnormalities of muscle tissue in mice with juvenile visceral steatosis associated with systemic carnitine deficiency

Received: 11 July 1994 / Accepted: 13 February 1995

Abstract A mouse with juvenile visceral steatosis (the JVS mouse) has been recognized as a novel animal model for systemic carnitine deficiency. We examined cardiac, skeletal and smooth muscle cells in JVS and control mice by light and electron microscopy. Cardiac and skeletal muscle cells of these mice at 4 weeks of age exhibited a ragged-red appearance after trichrome staining. Electron microscopy, demonstrated increased numbers of mitochondria and lipid droplets in the cells. Compression or distortion of the myofibril bundles, primarily due to the increased number of mitochondria, suggests the possible existence of a functional disturbance of the cardiac and skeletal muscle. In the urinary bladder, only one or two large lipid droplets and slightly increased number of mitochondria were recognized in the perinuclear region of the smooth muscle cells. At 8 weeks of age, the mouse enzyme histochemistry specific for mitochondria, such as cytochrome c oxidase and succinic dehydrogenase, and oil red O staining, confirmed further increases in the number of mitochondria and lipid droplets in the heart. However, the accumulation of these organelles in the skeletal and smooth muscle cells was no greater than that noted in JVS mice at 4 weeks of age. In the cardiac muscle cells, autolysosomes or autophagic vacuoles containing electron-dense membranous, lamellar or whorled structures closely associated with mitochondria and pseudoinclusion bodies in the nucleus were recognized, and bundles of myofibrils were buried under numerous mitochondria, suggesting the existence of disturbed contractile function in the heart of JVS mice. These results indicate that this murine strain associated with systemic carnitine deficiency exhibits a generalized mitochondrial abnormality in the muscle system especially in the heart.

Key words JVS mouse · Systemic carnitine deficiency · Mitochondrial abnormality · Ultrastructure

J. Miyagawa (✉) · M. Kuwajima · T. Hanafusa · A. Ono
R. Uenaka · T. Oue · K. Yamamoto · Y. Matsuzawa
Second Department of Internal Medicine,
Osaka University Medical School, 2-2 Yamadaoka,
Suita 565, Japan

K. Ozaki · I. Narama
Research Institute of Drug Safety, Setsunan University,
45-1 Nagaotoge-cho, Hirakata, Osaka 573-1, Japan

H. Fujimura · M. Kaidoh
Department of Neurology, Osaka University Medical School,
2-2 Yamadaoka, Suita 565, Japan

H. Nikaido · J. Hayakawa
Institute for Experimental Animals, School of Medicine,
Kanazawa University, Kanazawa 920, Japan

M. Horiuchi · T. Saheki
First Department of Biochemistry, Faculty of Medicine,
Kagoshima University, 8-35-1 Sakuragaoka,
Kagoshima 890, Japan

Introduction

Koizumi et al. [8] have reported a C3H.OH (formerly misnamed C3H-H-2°) strain of mouse associated with visceral microvesicular fatty infiltration which is inherited in an autosomal recessive manner. This mouse was later named the juvenile visceral steatosis (JVS) mouse [4]. At 3–28 days of age, the JVS mouse develops abnormal features including retarded growth and an enlarged abdomen. The activity of all urea cycle enzymes is very low in these mice, resulting in hyperammonaemia [7]. The similarity between JVS mice and patients with systemic carnitine deficiency prompted us to investigate the role of carnitine in pathogenesis of the model. Consequently, Kuwajima et al. [9] reported a marked decrease in carnitine concentrations in the serum, liver and muscle in JVS mice and established them as a model for systemic carnitine deficiency. Abnormalities in the expression of urea cycle enzymes abundant in the liver have been demonstrated [5, 13]. Tomomura et al. [14] have recently reported an increase in the levels of messenger RNAs encoding the proto-oncogenes c-*jun* and c-*fos*, α-fetoprotein and aldolase A, suggesting that the hepatocytes of JVS mice are in an undifferentiated or de-differentiated state.

Histological examinations of JVS mice showed lipid droplets in hepatocytes and in the epithelium of the proximal convoluted tubule of the kidney [8]. However, little data exist regarding the histological features of the muscle, one of the most affected organs. We therefore investigated the histological features in the myocardium, skeletal muscle cells and smooth muscle cells of the urinary bladder. This report details the marked histological abnormalities found in these organs.

Materials and methods

All animals were maintained under specific pathogen free conditions. Homozygous mutants designated jvs/jvs showed a swollen fatty liver through the abdominal wall at 2–5 days after birth and these mutants are the test JVS mice. Both normal homozygotes (+/+) and heterozygotes (+/jvs) served as controls, since they were indistinguishable. Eight JVS mice 4 weeks of age, ten JVS mice 8 weeks of age and eight age-matched control mice were examined. Age-matched C3H-OH mice, the original strain of JVS mice, were also studied.

The animals were anaesthetized by intraperitoneal injection of pentobarbital (0.025 mg/g body weight). For light microscopy, a portion of skeletal muscle (biceps femoris muscle), heart and urinary bladder were excised and quickly frozen in a dry ice isopentane bath. Frozen tissues were cut into 4–8 μm thick sections by cryostat and were examined after staining with haematoxylin and eosin (H&E), modified Gomori's trichrome (m-GT), succinic dehydrogenase (SDH), cytochrome c oxidase (CCO) and oil red O. For electron microscopy, mice were perfused via the ascending aorta with 3% glutaraldehyde solution buffered at pH 7.4 with 0.1 M Millonig's phosphate buffer. Heart, skeletal muscle (biceps femoris muscle) and urinary bladder were excised, cut into small pieces and fixed with the same fixative for 2 h at 4° C. After secondary fixation with 1% osmium tetroxide solution buffered at pH 7.4 with 0.1 M Millonig's phosphate buffer for 1 h at 4° C, specimens were dehydrated and embedded in Epon (epoxy resin). Ultrathin sections, cut on a Reichert-Jung Ultracut E ultramicrotome, were doubly stained with aqueous uranyl acetate (3.0%) and Reynold's lead citrate and were then observed using a Hitachi H-7000 electron microscope.

For quantitative electron microscopic morphometrical analysis, three blocks from cardiac tissues of each animal were randomly chosen (2, 4 and 8 weeks of age; four animals in each group), and photographs of 20 cardiac muscle cells including nucleus were taken from one block at an original magnification of ×2,000. The number of abnormal mitochondria with a highly electron-dense matrix (autolysosomes apparently derived from mitochondria) was counted on the prints at a final magnification of ×4,000. In addition, the total number of autolysosomes or autophagic vacuoles including mitochondria sequestrated by a lysosome was also counted. For statistical analysis, the unpaired Student's *t*-test was adopted, and P values <0.05 were considered to be statistically significant.

Results

Cardiac muscle cells

Light microscopy

At 4 weeks of age, morphological differences were difficult to observe between JVS mice and control of original C3H-OH mice on H&E staining. However, the m-GT staining demonstrated a ragged-red appearance in many cells of JVS mice, suggesting that this change was due to an aggregation of mitochondria. At 8 weeks of age, cardiac muscle cells became somewhat larger in size, and enlarged nuclei were recognized in many cells of JVS mice when compared with those of control or original C3H.OH mice (Fig. 1a, b). Lipid droplets were also increased in number and size (Fig. 1c, d). These cells showed a striking ragged-red appearance after m-GT staining (Fig. 2a, b), and mitochondrial enzymes including CCO and SDH were intensely stained (Fig. 2c–f).

Electron microscopy

At 4 weeks of age, mitochondria with many tubular cristae were round or had a short rod-like shape, and were relatively rich in cytoplasm when compared with mitochondria in age-matched control mice (Fig. 3b). In JVS mice many, but not all, cardiac muscle cells showed an increase in the number of mitochondria. Many mitochondria had a polygonal shape, possibly due to compression by the increased number of mitochondria and the matrix of some mitochondria of lower electron density. The number of lipid droplets was also increased in these cells (Fig. 3a). In contrast to the features of cardiac muscle cells of control mice, bundles of myofibrils in JVS mice appeared to be distorted or split, and the nuclei were often irregular in shape (Fig. 3a).

At 8 weeks of age, pseudoinclusion bodies containing various cell organelles and cytoplasmic materials appeared in many nuclei (Fig. 4), and the number of mitochondria and lipid droplets was markedly increased. In addition, mitochondria with highly electron-dense matrices were frequently observed (Fig. 5a). By the examination of serial ultrathin sections, such mitochondria were often found to be in close contact with lysosomes, or appeared to be fused with lysosomes, suggesting that they were a category of autolysosome (Fig. 5b). Furthermore, aggregates of mitochondria probably sequestrated by lysosomes were also observed, and these mitochondria showed various stages of degeneration (Fig. 6a). In some of the cardiac muscle cells examined at this age, a large aggregate of autophagic vacuoles containing mitochondria and some other cell organelles or cytomembrane components could be recognized (Fig. 6b). However, muscle fibre necrosis was rarely observed. The number of mitochondria of the type described above was markedly increased in JVS mice at 4 and 8 weeks of age when compared with that in control mice, and the number of such structures per 1,000 μm^2 cytoplasmic area was 3.30±2.63 at 4 weeks of age and 9.10±2.96 at 8 weeks of age in JVS mice, and 0.30±0.48 at 4 weeks of age and 2.1±0.88 at 8 weeks of age in control mice (values are the mean ±standard deviation; $P<0.01$, $P<0.01$, respectively; Fig. 7a). Quantitative morphometric analysis also revealed that autolysosomes or autophagic vacuoles in cardiac muscle cells of JVS mice were mainly derived from mitochondria, although the number of such structures in control mice was slightly increased at 8 weeks of

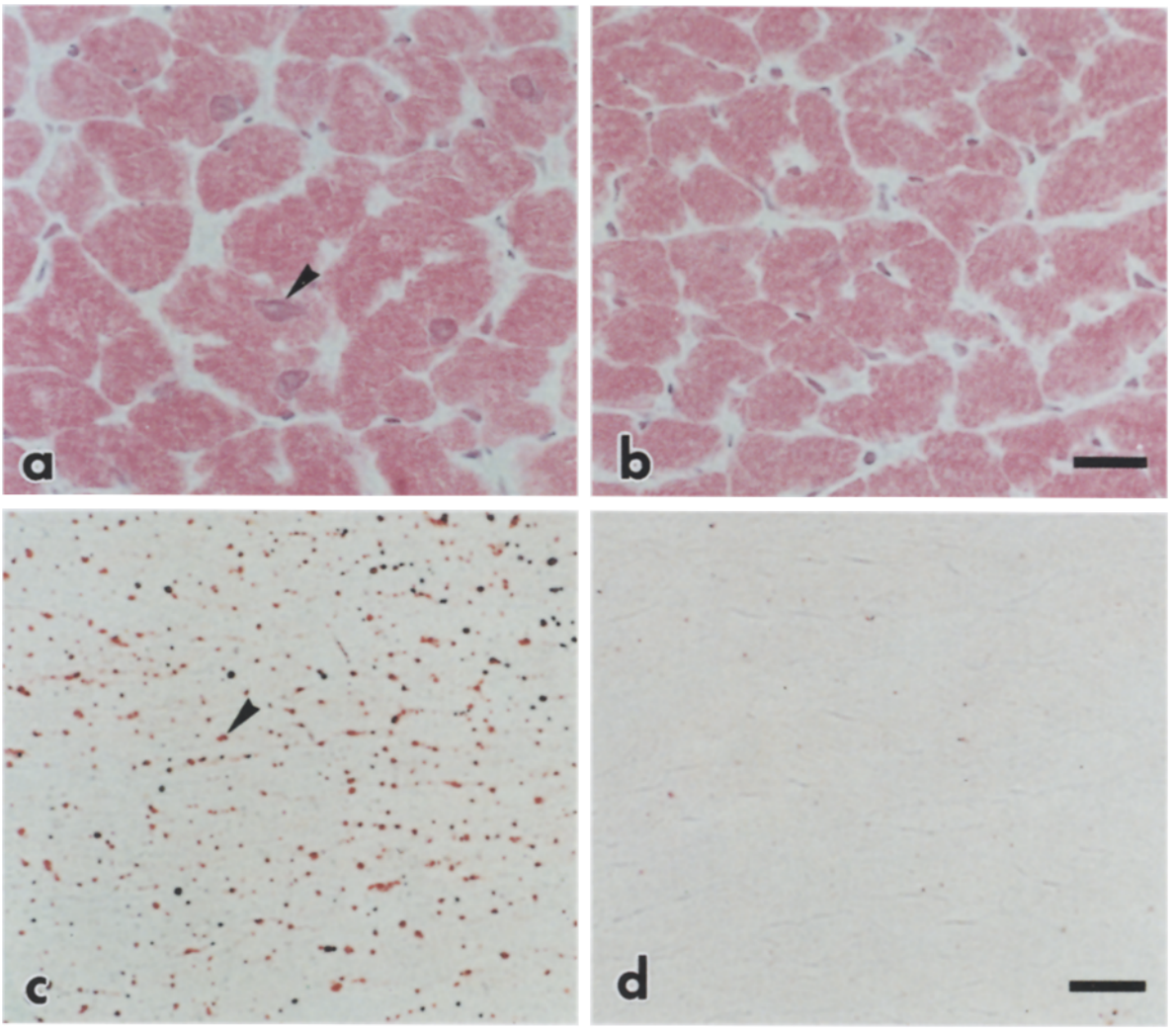

Fig. 1a–d Light micrographs of cardiac tissue from 8-week-old juvenile visceral steatosis (JVS) and control mice. Cardiac muscle cells of the JVS mouse (**a**) are slightly larger than those of the control mouse (**b**), and large nuclei (*arrow*) can be observed in the former. (Haematoxylin and eosin, ×490). **c**, **d** In the JVS mouse, many lipid droplets (red dots or spots, *arrowhead*) can be detected at this age, while such droplets cannot easily be recognized in the control mouse. (Oil red O, ×490. *Bar*=20 μm)

age when compared with that in control mice at 2 or 4 weeks of age (Fig. 7b).

Skeletal muscle

Light microscopy

At 4 weeks of age, the structure of skeletal muscle in JVS mice appeared to be normal as determined by observing tissue sections after H&E staining. Each muscle fibre had fine striations in longitudinal sections, and was round or polygonal in shape. The nuclei were located at the periphery in cross sections. However, m-GT staining revealed that many of the fibres of JVS mice showed a ragged-red appearance as seen in the cardiac muscle cells (data not shown). Oil red O staining showed excessive lipid accumulation among fibres. At 8 weeks of age, the morphological changes were essentially the same and there was no apparent muscle fibre degeneration or interstitial connective tissue proliferation.

Electron microscopy

Cellular organelles of muscle fibres in control mice had a normal ultrastructural appearance as noted in original C3H-OH mice at 4 and 8 weeks of age. The mitochondria with many tubular cristae were round or had a short rod-like shape. They were located between myofibrils, and in the perinuclear or subsarcolemmal region. Lipid droplets were observed scattered in the same regions. Myofibrils showed clear contractile units of sarcomeres. Dark-staining A bands and light-staining I bands could clearly be observed in longitudinal sections (Fig. 3d). In contrast, JVS mice at 4 weeks of age showed ultrastructural abnormalities in some organelles. There was a marked increase in the number of mitochondria (Fig. 3c). However, the mitochondrial matrix appeared to be virtually the same as

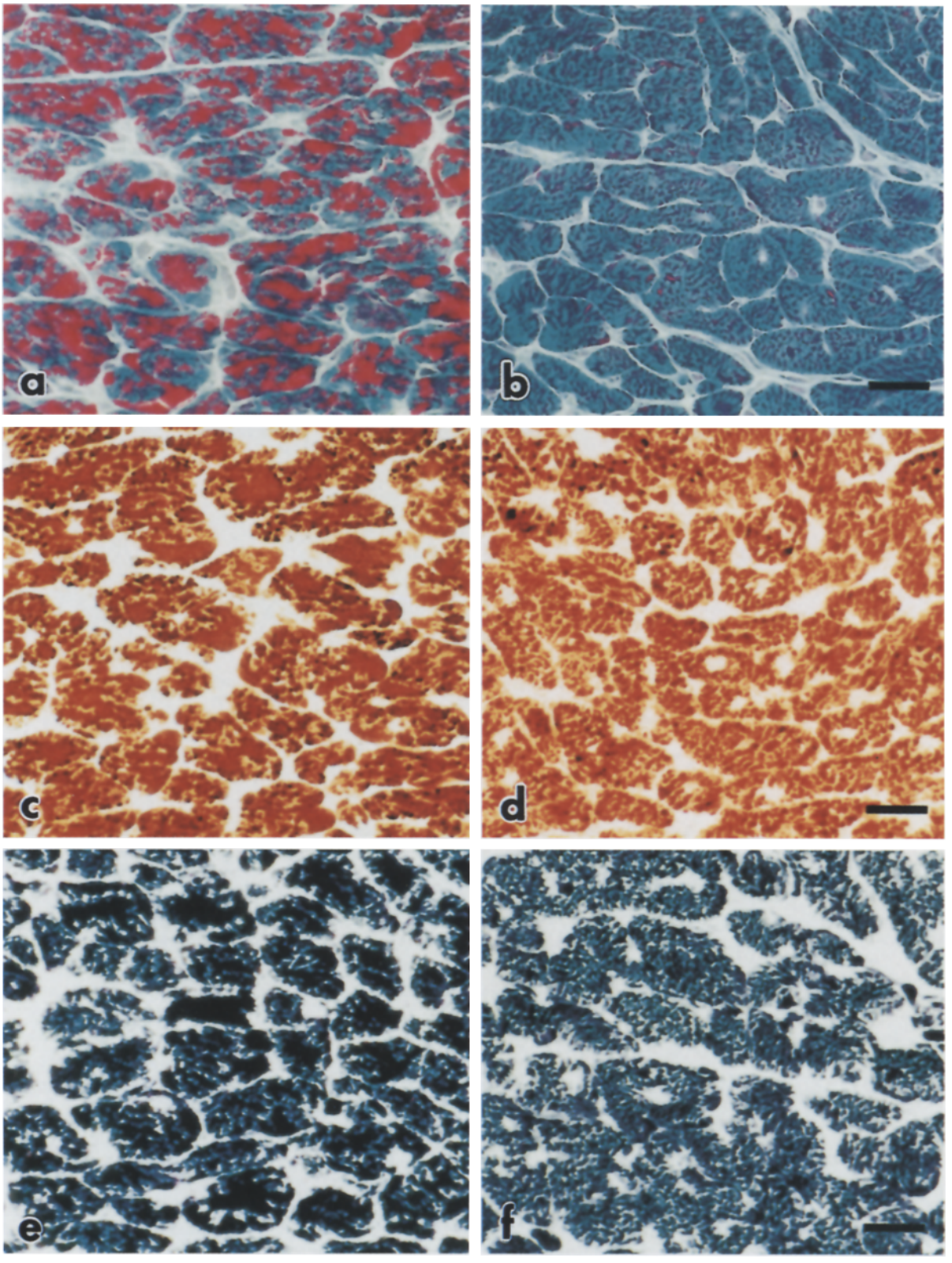

Fig. 2a–f Light micrographs of cardiac muscle tissue sections after histochemical staining by modified Gomori's trichrome (m-GT), cytochrome c oxidase (CCO) and succinic dehydrogenase (SDH) in 8-week-old JVS and control mice. **a**, **b** Cardiac muscle cells of the JVS mouse (**a**) show marked ragged-red appearance in transverse section. (Cryosections of 8 μm thickness, m-GT staining, ×490. *Bar*=20 μm). **c–f** In JVS mice, more intense staining of CCO and SDH (**c** and **e**, respectively) can be seen than in control mice (**d**, **f**). (Cryosections of 4 μm thickness. **c**, **d** CCO staining; **e**, **f** SDH staining; ×490. *Bar*=20 μm)

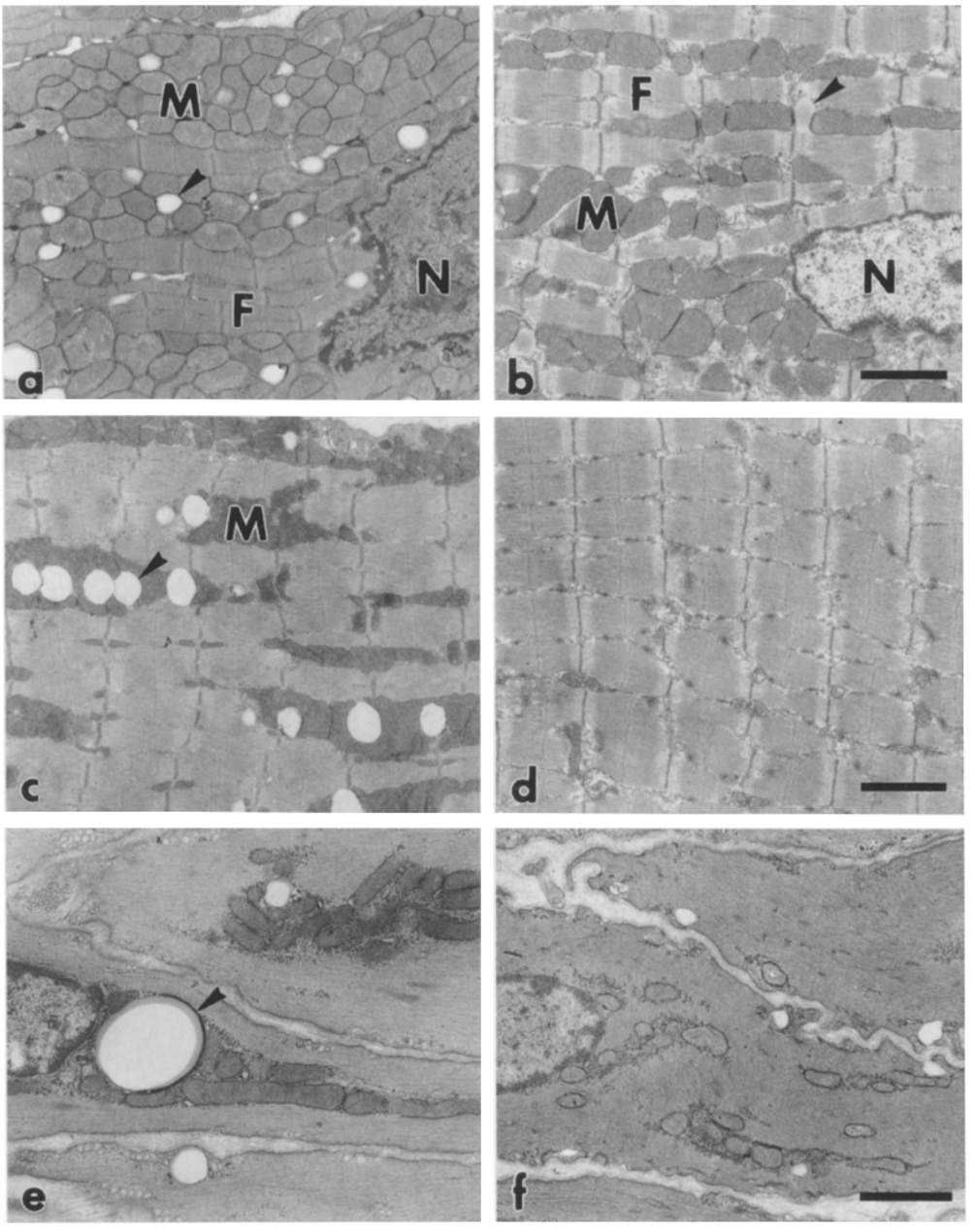

Fig. 3a–f Electron micrographs of cardiac, skeletal and smooth muscle cells in 4-week-old JVS and control mice. In a cardiac muscle cell of a 4-week-old JVS mouse (**a**), increased numbers of mitochondria (*M*) and lipid droplets (*arrowhead*) can be seen in the cytoplasm, and the nucleus (*N*) shows an irregular shape when compared with a cardiac muscle cell of a control mouse (**b**). Bundles of myofibrils (*F*) appear to be distorted and are buried under the numerous mitochondria in (**a**). In a cardiac muscle cell of the control mouse (**b**), mitochondria can be seen only between bundles of myofibrils, and in the perinuclear and subsarcolemmal region. Small-sized lipid droplets (*arrowhead*) can be observed, and bundles of myofibrils are seen running in an orderly fashion in the cytoplasm (**a**, **b** ×5,700. *Bar*=2 μm). A longitudinal section of skeletal muscle cells (biceps femoris) in the 4-week-old JVS mouse (**c**) also shows increased number of mitochondria localized between bundles of myofibrils, and in the subsarcolemmal space. Lipid droplets (*arrowhead*) are also increased in number and size, and exist among clusters of mitochondria. In a skeletal muscle cell of the control mouse (**d**), bundles of myofibrils run in a parallel fashion. A small number of mitochondria and glycogen particles can be seen between the bundles of myofibrils. (**c**, **d** ×5,700. *Bar*=2 μm). In smooth muscle cells of the urinary bladder in the 4-week-old JVS mouse (**e**), changes in the numbers of mitochondria and lipid droplets are not distinct, and only one or two large lipid droplets (*arrowhead*) in the perinuclear region can be seen closely associated with mitochondria. However, such large intracellular lipid droplets are not seen in smooth muscle cells of the urinary bladder in the control mouse (**f**). (**e**, **f** ×12,200. *Bar*=1 μm)

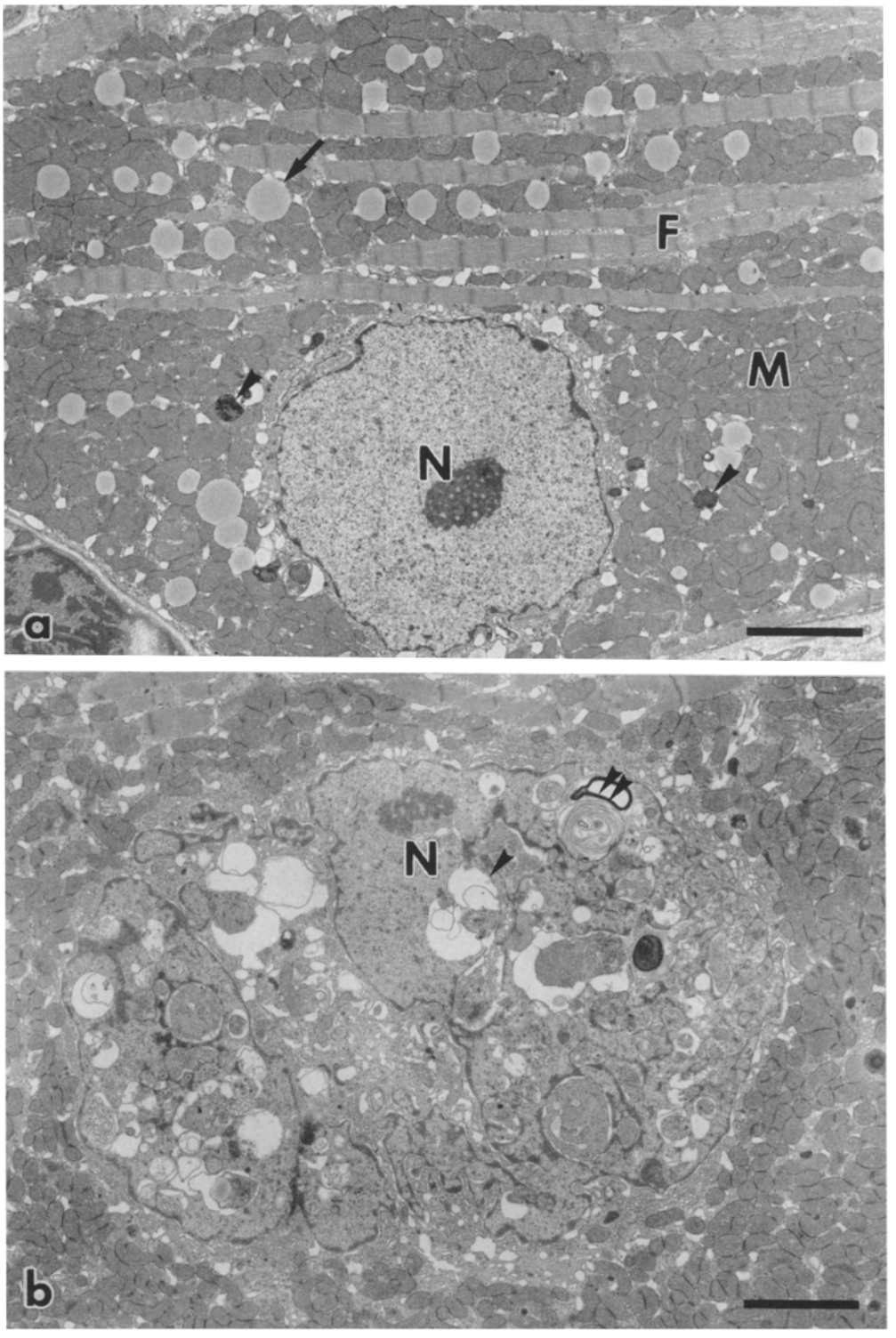

Fig. 4a, b Electron micrograph of a cardiac muscle cell of an 8-week-old JVS mouse. **a** Numerous mitochondria can be seen in the perinuclear region and between bundles of myofibrils. Lipid droplets (*arrow*), also increased in the number and size, exist among clusters of mitochondria. Electron-dense lysosome-like "granules" can be seen (*arrowhead*). (×5,600. *Bar*=3 μm). **b** Invaginated or distorted nuclei formed many pseudoinclusion bodies, in which various-sized vacuolar (*arrowhead*) or lamellar (*double arrowhead*) structures can be seen. (×4,200. *Bar*=2 μm)

in the muscle fibres of control mice with regard to electron density. Lipid droplets were also frequently seen in close association with clusters of mitochondria. The bundles of myofibrils were partially split or disrupted due to the increased numbers of mitochondria and lipid droplets (Fig. 3c). At 8 weeks of age, similar ultrastructural findings were observed in JVS mice and the degree of the mitochondrial accumulation and lipid droplet appeared to be very similar to that seen at 4 weeks of age.

Smooth muscle cells in the urinary bladder

No apparent differences were observed between the smooth muscle cells of the urinary bladder in JVS mice and those of control or original C3H.OH mice on light microscopy. However, electron microscopy demonstrated that one or two large lipid droplets were occasionally present in the perinuclear region of smooth muscle cells in 4-week-old JVS mice (Fig. 3e). Similar large lipid

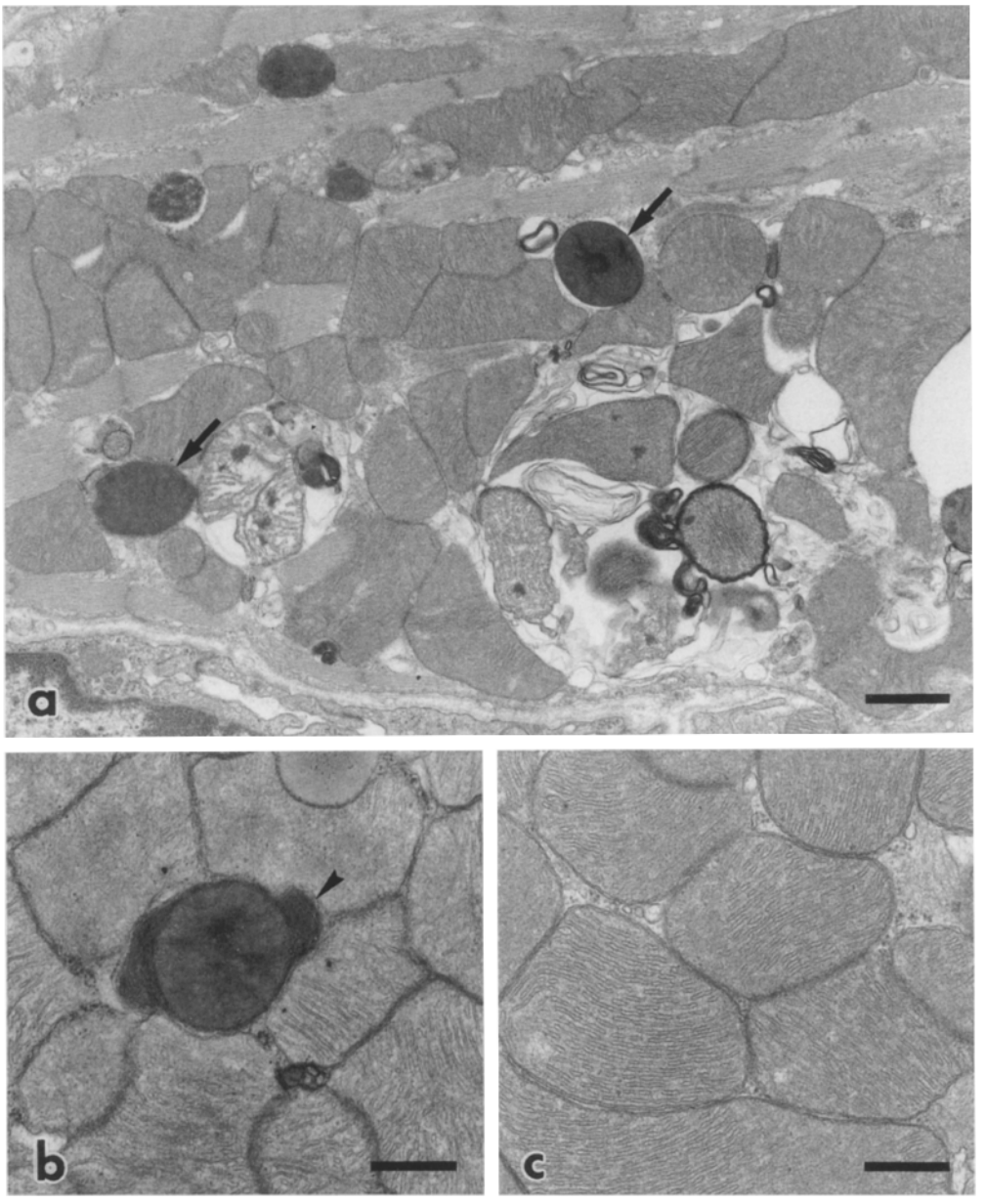

Fig. 5a–c Electron micrographs of abnormal mitochondria in a cardiac muscle cell of an 8-week-old JVS mouse. **a** Many mitochondria are irregular in shape, and regularly arranged mitochondrial cristae appear to be decreased. Mitochondria with highly electron-dense matrices show a lysosome-like appearance (*arrows*). (×11,400. *Bar*=1μm). **b** Mitochondrion sequestrated by a primary lysosome (*arrowhead*) show highly electron-dense matrix. Crista of the mitochondrion appear to be disorganized or partially digested. **c** Mitochondria of an 8-week-old control mouse demonstrate normal appearance with many regularly arranged cristae. (**b**, **c** ×22,800. *Bar*=0.5 μm)

droplets were not present in age-matched control or original C3H.OH mice (Fig. 3f). Lipid droplets were closely associated with mitochondria, but the ultrastructure of the mitochondria and other cyto-organelles appeared normal. These morphological changes were also the major findings in JVS mice at 8 weeks of age. The accumulation of mitochondria and lipid droplets in the smooth muscle cells was the least marked among the three types of muscle cells examined.

Discussion

The JVS mouse has been established as an animal model for systemic carnitine deficiency because of marked decrease of carnitine conçentrations in the serum, liver and skeletal muscles [9]. The carnitine concentration in the heart of JVS mice is also decreased, and the levels of carnitine content were about 10–20% of those in age-matched control mice (Kuwajima et al., in preparation).

In this study, we have demonstrated that cardiac and skeletal muscle cells of JVS mice showed increased number of lipid droplets. These cells also showed a marked increase in the number of mitochondria. In cardiac muscle cells, the accumulation of mitochondria became more remarkable with time. In addition to myofibrillar disarrangement, the appearance of pseudoinclusion bodies in the nucleus and autolysosomes or autophagic vacuoles which contained degenerating and/or degenerated mitochondria suggested the existence of disturbed contractile function in the heart of JVS mice. It is noteworthy that the increased numbers of lipid droplets in the muscle cells were always closely associated with the mitochondria. Since mitochondria contain many of the enzymes necessary for fat metabolism including fatty oxidases, the increased numbers of mitochondria and lip-

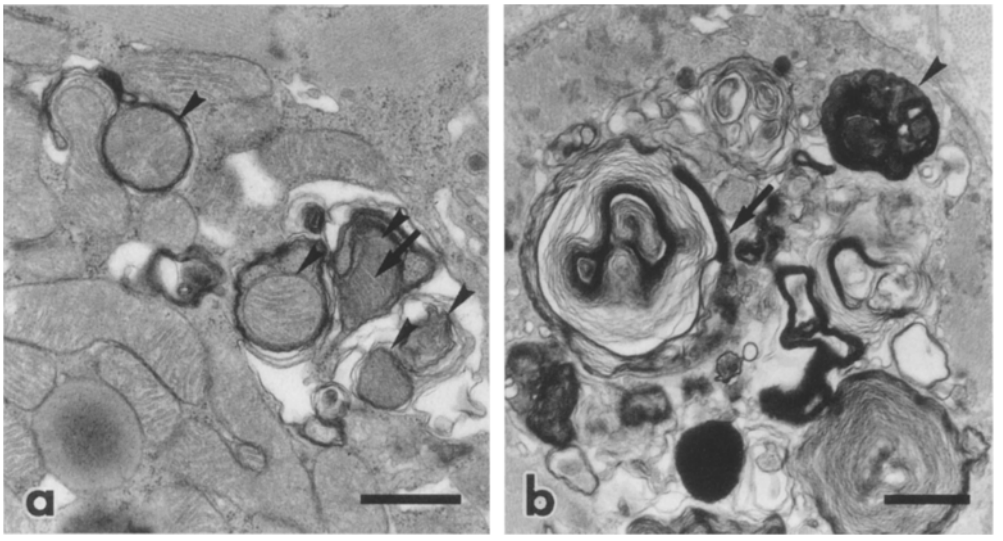

Fig. 6 Autolysosome or autophagic vacuoles seen in cardiac muscle cells of an 8-week-old JVS mouse. **a** Mitochondria surrounded by membraneous structures (*arrowheads*) were observed. These mitochondria showed various stages of degeneration, although crista of some mitochondria (*arrow*) can still be recognized. (×13,200. *Bar*=1 μm). **b** Autolysosomes or autophagic vacuoles were seen aggregating in the cytoplasm. Electron-dense autolysosome which include membrane-bound structures (*arrowhead*) and membranous, lamellar structures surrounded by lysosomes (*arrow*) were observed. (×22,600, *Bar*=0.5 μm)

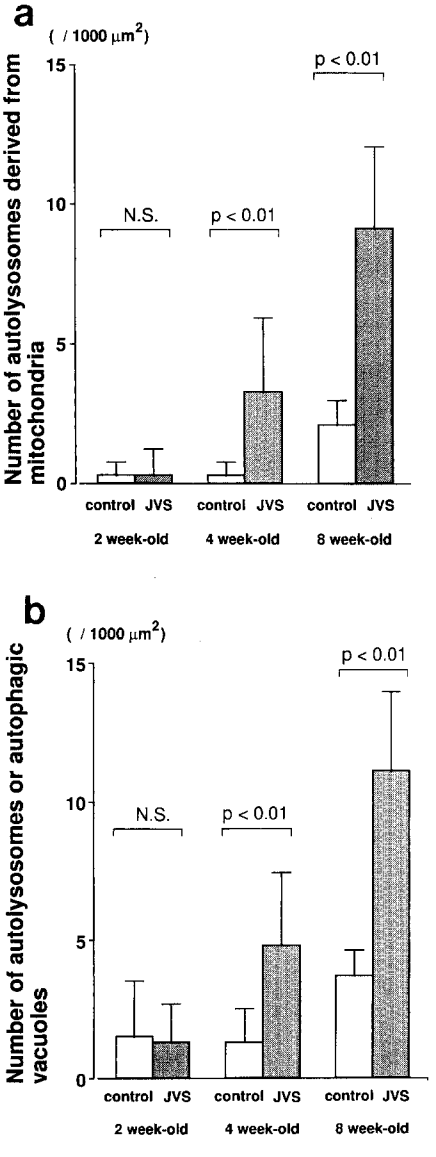

id droplets might reflect the abnormal mitochondrial function and/or lipid metabolism, whatever the cause. These changes were also observed in smooth muscle cells of the urinary bladder, but to a lesser degree.

Similar morphological changes have been observed in the skeletal muscle cells of patients with systemic carnitine deficiency. Major and diagnostic ultrastructural abnormalities can be seen in the skeletal muscle cells of patients with this disorder, and they are associated with increases in the number and size of mitochondria and accumulation of lipid droplets [2, 11]. Additionally, the cardiac muscle of patients with this disorder exhibits a lipid storage myopathy with hypertrophic cardiomyopathy [3]. Ultrastructurally, cardiac muscle cells in biopsy specimens display excessive numbers of lipid droplets and ag-

Fig. 7 The number of autolysosomes derived from mitochondria (**a**), and the total number of autolysosomes or autophagic vacuoles (**b**) in cardiac muscle cells of JVS and control mice. **a** The number of autolysosomes derived from mitochondria which showed highly electron-dense matrices in 2-week-old JVS mice was almost the same as that in 2-week-old control mice. However, these autolysosomes were significantly increased in number in 4-week-old JVS mice. At 8 weeks of age, the number of such structures in cardiac muscle cells of JVS mice was further increased, although a slight increase in the number of autolysosomes derived from mitochondria was observed in 8-week-old control mice compared to that observed in 2- or 4-week-old control mice. (*N.S.* not significant). **b** The total number of autolysosomes or autophagic vacuoles, including autolysosomes derived from mitochondria, observed in cardiac muscle cells of 4- and 8-week-old JVS mice was significantly increased compared to those in age-matched control mice. Comparison of **a** and **b** revealed that a marked increase in the number of autolysosomes derived from abnormal mitochondria in cardiac muscle cells of 4- and 8-week-old JVS mice was responsible for the increase in the total number of autolysosomes or autophagic vacuoles. The uncountable aggregated autolysosomes or autophagic vacuoles, each of which was difficult to discriminate due to degeneration, were counted as one autolysosome or autophagic vacuole. Each column is the mean for four animals in each group ± standard deviation

gregates of mitochondria [10]. These findings are very similar to those found in the present study in the muscles of the JVS mouse, although a ragged-red appearance of muscle fibres is unusual in human carnitine deficiency.

The systemic carnitine deficiency occurs in some inherited metabolic disorders, particularly those of β-oxidation, such as medium-chain acyl CoA dehydrogenase deficiency [1] and defects of renal tubular reabsorption [12]. Western blot analysis showed no primary abnormalities of the enzymes involved in mitochondrial β-oxidation in JVS mice (Hashimoto T, personal communication), and the results of histochemical staining for CCO and SDH further suggest that there may be no major primary defect in mitochondrial function, although a mitochondrial defect of the respiratory chain cannot be excluded.

A primary defect in carnitine metabolism in the JVS mouse has not yet been defined. However, we have recently demonstrated that the systemic carnitine deficiency found in the JVS mouse may be due to a defect in the renal carnitine transport system [6]. Since carnitine acts as an essential cofactor in the transport of long-chain fatty acids into mitochondria, the morphological changes reported here may be of use in understanding the clinical features of patients with systemic carnitine deficiency, especially those with a defect in the renal carnitine transport system.

This report is the first to describe the abnormal morphological changes, particularly those of the mitochondria, in the muscle system of carnitine deficient mice. Although further investigation will be necessary to clarify the pathological features of various organs in these mice, this study has demonstrated the usefulness of the JVS mouse as a model of human systemic carnitine deficiency.

Acknowledgements This study was supported in part by a grant (No. 04671476) from the Ministry of Education, Science and Culture of Japan. The authors wish to express their thanks to Ms. K. Yamamori for her technical assistance.

References

1. Engel AG (1986) Carnitine deficiency syndromes and lipid storage myopathies. In: Engel AG, Banker BQ (eds) Myology (vol 2). McGraw-Hill Book Company, New York, pp 1633–1693
2. Engel AG, Angelini C (1973) Carnitine deficiency of human skeletal muscle with associated lipid storage myopathy: a new syndrome. Science 179:899–901
3. Galen NB (1990) Carnitine deficiency syndromes. Pediatr Neurol 6:75–81
4. Hayakawa J, Koizumi T, Nikaido H (1990) Inheritance of juvenile visceral steatosis (jvs) found in C3H-H-2° mice. Mouse Genome 86:261
5. Horiuchi M, Kobayashi K, Tomomura M, Kuwajima M, Imamura Y, Koizumi T, Nikaido H, Hayakawa J, Saheki T (1992) Carnitine administration to juvenile visceral steatosis mice corrects the suppressed expression of urea cycle enzymes by normalizing their transcription. J Biol Chem 267:5032–5035
6. Horiuchi M, Kobayashi K, Yamaguchi S, Shimizu N, Koizumi T, Nikaido H, Hayakawa J, Kuwajima M, Saheki T (1994) Primary defect of juvenile visceral steatosis (jvs) mouse with systemic carnitine deficiency is probably in renal carnitine transport system. Biochim Biophys Acta 1226:25–30
7. Imamura Y, Saheki T, Arakawa H, Noda T, Koizumi T, Nikaido H, Hayakawa J (1990) Urea cycle disorder in C3H-H-2° mice with juvenile steatosis of viscera. FEBS Lett 269:119–121
8. Koizumi T, Nikaido H, Hayakawa J, Nonomura A, Yoneda T (1988) Infantile disease with microvesicular fatty infiltration of viscera spontaneously occurring in the C3H-H-2° strain of mouse with similarities to Reye's syndrome. Lab Anim 22: 83–87
9. Kuwajima M, Kono N, Horiuchi M, Imamura Y, Ono A, Inui Y, Kawata S, Koizumi T, Hayakawa J, Saheki T, Tarui S (1991) Animal model of systemic carnitine deficiency: Analysis in C3H-3-2° strain of mouse associated with juvenile visceral steatosis. Biochem Biophys Res Commun 174:1090–1094
10. Matsuishi T, Hirata K, Terasawa K, Kato H, Yoshino M, Ohtaki E, Hirose F (1985) Successful carnitine treatment in two siblings having lipid storage myopathy with hypertrophic cardiomyopathy. Neuropediatrics 16:6–12
11. Petrykowski W, Ketelsen U, Schmidt-Sommerfeld E, Penn D, Sawicka E, Struck E, Lehnert W, Haap K, Strassburg H (1985) Primary systemic carnitine deficiency under successful therapy: clinical, biochemical, ultrahistochemical and renal clearance studies. Clin Neuropathol 4:63–71
12. Rodrigues PR, Schlotte HR, Luyt-Houwen IEM, Vaandrager-Verduim MHM (1988) Cardiomyopathy associated with carnitine loss in kidneys and small intestine. Eur J Pediatr 148: 193–197
13. Tomomura M, Imamura Y, Horiuchi M, Koizumi T, Nikaido H, Hayakawa J, Saheki T (1992) Abnormal expression of urea cycle enzyme genes in juvenile visceral steatosis (jvs) mice. Biochim Biophys Acta 1138:167–171
14. Tomomura M, Nakagawa K, Saheki T (1992) Proto-oncogene c-*jun* and c-*fos* messenger RNAs increase in the liver of carnitine-deficient juvenile visceral steatosis (jvs) mice. FEBS Lett 311:63–66